





## Research Article

# Green Synthesis of Iron Nanoparticles: Application on the Removal of Petroleum Oil from Contaminated Water and Soils

Erika Murgueitio <sup>1,2</sup> Luis Cumbal <sup>1,3</sup> Mayra Abril,<sup>1</sup> Andrés Izquierdo <sup>1,3</sup>  
Alexis Debut <sup>1,3</sup> and Oscar Tinoco<sup>2</sup>

<sup>1</sup>Centro de Nanociencia y Nanotecnología, Universidad de las Fuerzas Armadas ESPE, Av. Gral. Rumiñahui s/n, P.O. Box 171-5-231B, Sangolquí, Ecuador

<sup>2</sup>Unidad de Posgrado, Facultad de Ingeniería Geológica, Minera, Metalúrgica y Geográfica, Doctorado en Ciencias Ambientales, Universidad Nacional Mayor de San Marcos, Lima, Peru

<sup>3</sup>Departamento de Ciencias de la Vida y de la Agricultura, Universidad de las Fuerzas Armadas ESPE, Av. Gral. Rumiñahui s/n, P.O. Box 171-5-231B, Sangolquí, Ecuador

Correspondence should be addressed to Erika Murgueitio; [esmurgueitio@espe.edu.ec](mailto:esmurgueitio@espe.edu.ec)

Received 4 March 2018; Revised 20 June 2018; Accepted 14 July 2018; Published 2 September 2018

Academic Editor: Carlos R. Cabrera

Copyright © 2018 Erika Murgueitio et al. This is an open access article distributed under the Creative Commons Attribution License, which permits unrestricted use, distribution, and reproduction in any medium, provided the original work is properly cited.

Iron nanoparticles were produced using the extract of mortiño berry (*Vaccinium floribundum*) (vZVI) as reducing and stabilizer agent. Fresh nanoparticles were characterized using TEM, XRD, and FTIR techniques, while laboratory experiments were conducted to assess the removal of total petroleum hydrocarbons (TPHs) from water and soil after treatment with synthesized nanoscale iron particles. Nanoparticles as produced were spherical in the range of 5–10 nm. After treatment with vZVI nanoparticles, water contaminated with two concentrations of TPHs (9.32 mg/L and 94.20 mg/L) showed removals of 85.94% and 88.34%, respectively, whereas a contaminated soil with a TPHs concentration of 5000 mg/kg treated during 32 h with nanoparticles reached a removal of 81.90%. Results indicate that the addition of vZVI nanoparticles produced strong reducing conditions, which accelerate removal of TPHs and suggest that these nanoparticles might be a promising technology to clean up TPHs contaminated water and soils.

## 1. Introduction

Total petroleum hydrocarbons (TPHs) encompass a broad family of several hundreds of chemical compounds that originally come from crude oil [1]. These nature-based hydrocarbons embody a group of persistent organic contaminants [2], which pollute different environmental compartments such as air, water, soils, and sediments, and cause a probable toxic impact on different biological receptors [3]. The strategies employed to remediate soils contaminated with hydrocarbons can be physical, chemical, and biological processes [4, 5]. However, these techniques have shown drawbacks due to high cost, long-term treatment, difficulty in reducing the concentration of pollutants to the regulated levels, and ability to reach the contaminant

in the subsurface [6, 7]. Recently, a new experimental setup has been proposed using iron nanoparticles [8]. Remediation of soils with engineered nanomaterials (ENMs) promises more effective and cheaper approaches than conventional methods because of the increased reactivity of nanoparticles and the possibility of *in situ* treatment [9]. Microscale granular metallic iron (mZVI) has been widely used as a reducing agent for the remediation of a variety of contaminants in permeable reactive barriers. However, the cost of this method is deemed high and the process extent could be approximately 15 years [10]. Also, zerovalent iron nanoparticles have been successfully used in the past to remediate groundwater. Due to its small size and large surface area per unit mass, properties of the nanoparticles can be useful in hazardous waste site remediation and

contaminant reduction [11, 12]. Nevertheless, almost all tiny particles are prepared with toxic chemicals or require high capital costs and also generate hazardous toxic wastes. To overcome these shortcomings, this study examines an environmental friendly way to synthesize zerovalent iron nanoparticles using an endemic fruit from Ecuador, mortiño berry (*Vaccinium floribundum*). This fruit contains large amounts of polyphenols that are biodegradable and soluble in water at room temperature and have molecules carrying alcoholic functional groups that can be used for the reduction as well as for the stabilization of the nanoparticles [13]. In this work, peel and pulp of the fruits were used to obtain high concentration of polyphenols and high antioxidant capacity. The iron nanoparticles were synthesized by a simple procedure using the extract of mortiño berry to produce zerovalent nanoparticles iron from solutions of ferric ions. As-fabricated nanoparticles were then applied for the degradation of TPHs from contaminated water and soils.

## 2. Materials and Methods

**2.1. Materials.** In this study, a soil from the Ecuadorian Amazon region, La Joya de los Sachas County, Francisco de Orellana province, was collected to investigate TPHs remediation using vZI. For soil sampling, the protocol suggested in [14] was used. Concisely, a 500 m<sup>2</sup> of soil surface was divided into 5 × 5 m<sup>2</sup> squares. At the center point of each square, using an auger for soil drilling, 0.5 kg of soil was taken at a depth of 30 cm. Plant materials and stones were removed before mixing all soil samples. Then 4 kg of the mixed soil were taken for the study, stored in labeled ziploc plastic bags, and transported to the laboratory in a freezer at 4°C. Absolute ethanol and iron chloride (FeCl<sub>3</sub>·6H<sub>2</sub>O, 99.8%) were purchased from Scharlau and Fisher Scientific, respectively. A sample of petroleum hydrocarbons (22° API (American Petroleum Institute)) was obtained from the Joya de los Sachas Petroleum Storage Station, Ecuador. Double deionized water was produced using a Thermo Scientific Smart 2 pure deionized system.

### 2.2. Fabrication of Nanoparticles

**2.2.1. Extraction of Liquid Mortiño.** Fruit extract of *V. floribundum* (peel and pulp) was prepared by maceration with ethanol and magnetic stirring for 48 h in darkness. To minimize the passage of particles, the fruit extract was filtered three times through a filter paper of 1 mm diameter and a filter millipore millex-GV hydrophilic PVDF of 0.22 μm. Lastly, the extract was concentrated on a rotary evaporator (Buchi-850) removing the solvent.

**2.2.2. Polyphenol and Antioxidant Capacity Tests.** The polyphenol concentration of the extract was found with the Folin–Ciocalteu method. Briefly, the extract was sonicated on a CV33-Daigge ultrasonic processor and concentrated on a rotary evaporator. Thereafter, the polyphenol concentration was estimated. The antioxidant capacity was obtained, following the protocol developed by Brand-Williams et al. [15].

This method is based on the absorbance reduction of the antioxidant, measured at 515 nm for the DPPH radical. The concentration of DPPH in the reaction medium was calculated from a calibration curve obtained by linear regression. The results were expressed as activity equivalent to trolox (AET) (μM/g of fresh weight sample).

**2.2.3. Synthesis of Zerovalent Nanoparticles Using *V. floribundum* (vZVI).** Solutions of 0.5, 0.1, and 0.001 M of FeCl<sub>3</sub> were prepared as precursors of zerovalent iron. The extract of *V. floribundum* with a fixed pH between 9 and 10 was added to solutions of FeCl<sub>3</sub> at the volume ratio of 2:1 under sonication. The development of a black precipitate in the flask was an indication of the zerovalent nanoparticle formation, in all cases. Moreover, powder zerovalent nanoparticles were prepared by water evaporation, placing the liquid solution on a hot plate (DLab M57-H550-5). Additional drying of the wet solution was performed with a line of nitrogen gas in a fume hood for two hours. Finally, the solid sample was washed several times with deionized water to remove sodium chloride crystals.

**2.3. Characterization of Iron Nanoparticles.** Mineral composition of the nanoparticles was analyzed with a X-ray diffractometer (EMPYREAN, PANalytical) with 2θ configuration (generator-detector) wherein a copper disc emits X-rays at a wavelength of λ = 1.54 Å. For size distribution of nanoparticles, a submicron particle analyzer (HORIBA LB-550) was employed. Transmission electron microscope (TEM) images were digitally recorded for morphological studies (Tecnai G2 Spirit TWIN, FEI, Netherlands). The functional groups of the extract and the nanoparticles covered with the extract were recorded on a Spectra Two IR spectrometer (PerkinElmer, USA) and by UV-Vis (Analytik Jena).

**2.4. Batch Experiments to Remove TPHs from Contaminated Water and Soil Using vZVI Nanoparticles.** Laboratory experiments were performed following published protocols [16–18]. For the removal of TPHs dissolved in water, 1 g of vZVI was placed in amber-colored Boeco bottles filled with 100 mL of water containing 10 and 100 mg/L of TPHs in triplicate. Samples were stirred for 10 min in a Branson 3510 sonicator at amplitude of 70%. The supernatant was centrifuged, filtered, and sent for TPHs analysis in an accredited laboratory. TPHs removal from soils was performed following the procedure developed by Chang et al. [17] with some modifications. First, a series of 10 g soil samples were placed into 250 mL amber borosilicate glass bottles sealed with Teflon-lined screw caps. Petroleum was dissolved completely in hexane, and the solution was immediately poured into the bottles and then mixed for 2 h. Vial caps were left open in a fume hood for 8 h at ambient temperature to allow hexane evaporation thus resulting in homogeneous distribution of petroleum in the soil samples with 5000 mg TPHs/kg soil. Immediately, a solution of vZVI was added into the bottles containing the petroleum-spiked

soil at a ratio of 1:9 (w/v). Subsequently, the samples were sonicated for 20 min and shaken for 64 h, and the aqueous supernatant was decanted. The extraction of the petroleum residual was performed mixing the treated soil with dichloromethane (125 mL) and sonicated (Cole-Parmer, Model 08855-10). The extract was then filtered and analyzed for TPHs.

**2.5. Analytical Methods.** Total petroleum hydrocarbons were analyzed using a gas chromatograph (PerkinElmer Clarus, Model 400) equipped with a flame detection system (FID), capillary columns, and electronic pressure control split/splitless. Sample injection was carried out manually, and the running time for samples was fixed in 27 min. Equipment preparation and measurements were performed with Software Navigator TotalChrom Ver 6.3.1. For analytical validation, some samples were sent to an accredited laboratory for TPHs analysis.

### 3. Results and Discussion

**3.1. Polyphenol Content and Antioxidant Capacity.** Polyphenols in mortiño berry extract was found to be  $2127 \pm 805$  mg GAE/100 g sample. The content of polyphenols is similar to those found by Murgueitio et al. [19]. The antioxidant capacity of the fruit extract was measured as 50  $\mu$ mol trolox/g of sample (fresh weight), and this value is similar to those found by other authors [20–22].

**3.2. Visual and UV-Vis Study.** Figure 1 shows the absorption spectrum of the mortiño extract and the nanoparticles formation versus time. For the extract alone, it is observed a broaden peak between 570–585 and 610 nm due to the presence of anthocyanins (galloyl esters, hydroxybenzoic acid derivatives, flavan-3-ols, proanthocyanidins, flavonols, hydroxycinnamic acid derivatives, and anthocyanins) [23]. The biosynthesis of vZVI was monitored periodically at 2, 4, 6, and 8 h. It is observed that, in comparison with the brown-yellow  $\text{FeCl}_3$ , the color of the colloidal solution changed to blackish after the addition of the fruit extract. This is a direct proof for the reduction of  $\text{Fe}^{3+}$  to  $\text{Fe}^0$  and the formation of vZVI. The UV-Vis spectra indicate the disappearance of the extract peak when this interacts with the inorganic reagents during the growth of the nanoparticles as the time increases. This is because the structure of the polyphenols of the mortiño extract underwent changes throughout the synthesis of nanoparticles, forming aggregates of vZVINPs in the range of 5–35 nm. This trend is also associated with the high pH used in the preparation process of the nanoparticles [24, 25].

**3.3. Characterization of Nanoparticles.** Figure 2 shows TEM images of nanoparticles prepared with mortiño. As seen in the figure, particle sizes are in between 5 and 35 nm in diameter. Using statistical and algorithmic calculations developed by Arroyo et al. [26], nanoparticle diameters were also estimated. The highest percentage of formed vZVI

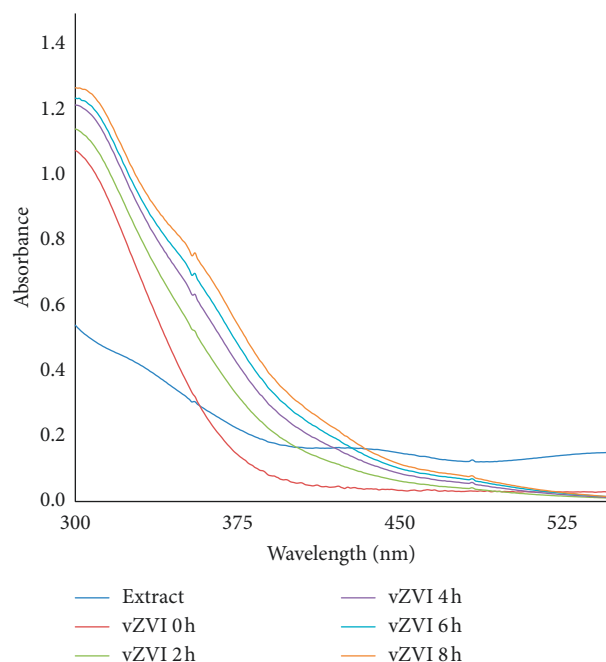


FIGURE 1: UV spectra of extract (*V. floribundum*) and vZVI.

nanoparticles in relation to 0.001 M  $\text{FeCl}_3$  is 61% for 5–10 nm in diameter while the lowest percentage is 3% for 30–35 nm (Table 1). On the contrary, with 0.1 M  $\text{FeCl}_3$ , the highest percentage is 45% for 15–20 nm and the lowest is 2% for 30–35 nm. Thus, calculated sizes of nanoparticles are in the range of 5 to 35 nm as well.

The mineral structure of the nanomaterials was characterized using XRD. Figure 3 shows the XRD pattern of synthesized vZVI nanoparticles. The major Bragg reflection at  $2\theta$  values are  $45.2537^\circ$ ,  $65.9598^\circ$ , and  $83.6821^\circ$  which correspond to the planes (110), (200), and (211) of  $\alpha\text{Fe}$  crystalline (code 98-042-6989 Fe1) with a body-centered cube crystal structure (bcc). The mineral composition of the fabricated nanoparticles is similar to those reported before by Murgueitio et al. [19]. Besides, XRD results revealed the as-produced nanoparticles contain 24% of metallic iron.

Finally, FTIR measurements were carried out to understand the contribution of the mortiño berry extract molecules in the formation of nanoparticles. As seen in Figure 4(a) and Table 2, peaks in the range of  $3650\text{--}3200\text{ cm}^{-1}$  are related to the vibrations of the  $\text{--OH}$  groups of the phenolic moiety of mortiño berry extract, positions from  $1620$  to  $1690\text{ cm}^{-1}$  are attributed to the aldehydes ( $\text{C=O}$ ) of an ester sugar [27]. These peaks in conjunction with the  $1089\text{ cm}^{-1}$  peak (CO stretching) represent the amount of carbon that belongs to the extract [28]. Conversely, for the nanoparticles, peaks of  $\text{C=C}$  alkene conjugate cis and benzene ring  $1634.98\text{ cm}^{-1}$  can be seen [23]. In addition, bands belonging to the goethite phase ( $\alpha\text{-FeO (OH)}$ ) with its vibration of the  $\text{Fe-O}$  bond in stretching mode are seen at  $630\text{ cm}^{-1}$  [29]. Thus, these groups may have participated in the nanoparticles synthesis. Hence, FTIR analysis confirms the presence of phenolic compounds and anthocyanins in mortiño berry extract, and



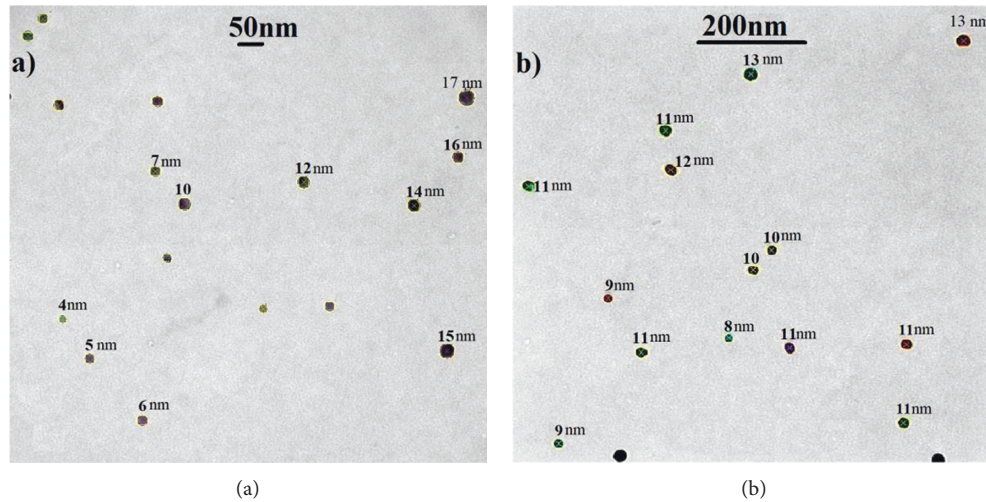


FIGURE 2: TEM images of vZVI.

TABLE 1: Percentage of vZVI produced in relation to the  $\text{FeCl}_3$  concentration.

Diameter range	0.001 M $\text{FeCl}_3$ (%)	0.1 M $\text{FeCl}_3$ (%)
5–10	61	3
10–15	12	21
15–20	9	45
20–25	12	19
25–30	4	10
30–35	3	2

further it acts as reducing/capping agents for the functionalization of vZVI.

**3.4. Treatment of Water Contaminated with TPHs Using vZVI Nanoparticles.** The chromatograms in Figures 5(a)–5(d) show the distribution of TPHs peaks in water before and after treatment with vZVI, respectively. Calculated percentages of TPHs removal are 85.94% ( $C_{\text{TPHs},f} = 9.32 \text{ mg/L}$  and  $C_{\text{TPHs},i} = 1.31 \text{ mg/L}$ ) and 88.34% ( $C_{\text{TPHs},f} = 94.20 \text{ mg/L}$  and  $C_{\text{TPHs},i} = 26.80 \text{ mg/L}$ ). It is observed in Figure 5(b) that peaks in the range of 7.5 min to 8 min and beyond 8.2 min disappear, compared to Figure 5(a). Besides, the long peak at 8.2 min remains after treatment because this corresponds to ortho-terphenyl, the compound that is used as a surrogate for quality control. The same tendency is observed in Figures 5(c) and 5(d) (for high TPHs concentration); however, peaks in Figure 5(d) (after treatment) are shorter compared to peaks in Figure 5(c) (before treatment). It is further observed in Figures 5(a) and 5(b) that compounds with C7–C10 carbons may volatilize because peaks are absent. The performance of nanomaterials in the removal of TPHs can be attributed to their increased surface area, and higher reactivity, and the possibility of in situ treatment.

**3.5. Treatment of Soils Contaminated with TPHs Using vZVI Nanoparticles.** Results show that vZVI with 24% of zerovalent iron removed 81.90% of petroleum hydrocarbons from soil after 32 h of treatment ( $C_{\text{TPHs},f} = 5000 \text{ mg/kg}$  and

$C_{\text{TPHs},i} = 931.8 \text{ mg/kg}$ ). Removal of TPHs from soils can be attributed to the high reactivity and sorption of the nanoparticles [9], as shown in Figure 6, zone a. The reducing power of the iron nanoparticles is provided by its core, which is mainly composed of zerovalent iron. The coverage of the nanoscale particles contains iron oxides and hydroxides that supply reactive sites for the immobilization of large petroleum hydrocarbons and the formation of chemical complexes (Figure 6, zone b). Measurements of TPHs in soil after 40, 56, and 64 h of treatment were also performed (inset Figure 6). It shows no more TPHs removal, indicating that the treatment reached steady state. A previous study has shown that 70% reduction of pyrene contained in soil samples was achieved in 60 min by contacting the soil with nanoscale ZVI powders in aqueous solution under ambient conditions with no pH control (Chang et al. [16]). Our treatment takes more time because TPHs are a cocktail of hundred derivatives with different molecular weight, size, viscosity, solubility, hydrophobicity, and so on, which may influence in the removal.

The removal mechanism of TPHs from water and soils using the vZVI could be a Fenton reaction. In the preparation of nanoparticles, it was used ultrasonication, as a result of this process, water of the iron solution could be splitted and produce hydrogen peroxide, although in small quantities [30, 31] (Equation (1)):



Fenton oxidation process starts when oxygenated water is activated with ferrous ions ( $\text{Fe}^{2+}$ ) coming from the oxidation of  $\text{Fe}^0$  nanoparticles.  $\text{Fe}^{2+}$  is in turn is oxidized to  $\text{Fe}^{3+}$ , producing hydroxyl ions and radicals. Then,  $\text{Fe}^{3+}$  is reduced to  $\text{Fe}^{2+}$  with hydrogen peroxide producing hydronium ions and peroxydril radicals,  $\text{OH}_2^*$  (Equations (2) and (3)). The radicals oxidize organics by abstraction of protons and producing organic radicals ( $\text{R}^*$ ) as shown in (4), which are highly reactive and can be further oxidized (Equations (5)–(7)) [32].

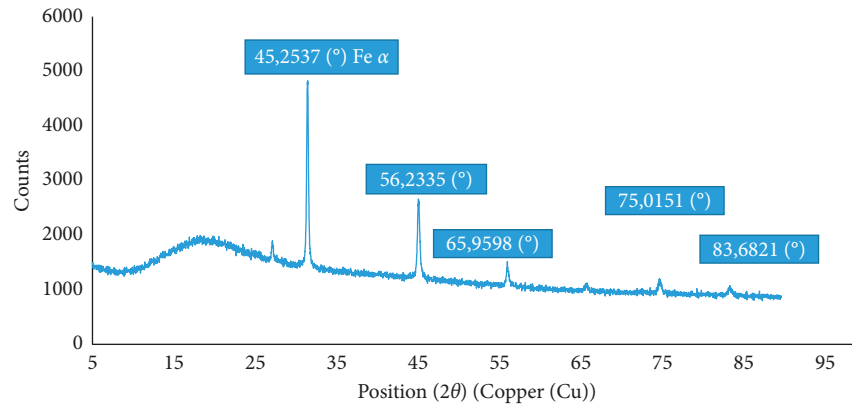


FIGURE 3: XRD pattern of iron nanoparticles prepared with mortiño berry (vZVI).

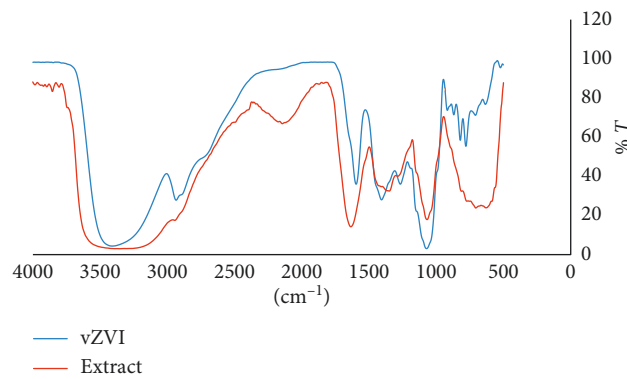
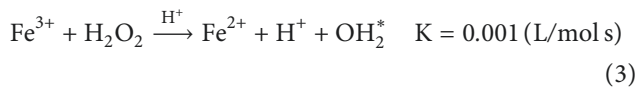
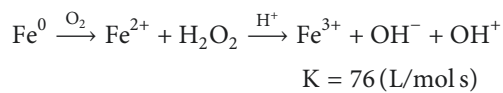
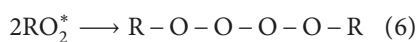
FIGURE 4: FTIR spectra of vZVI nanoparticles and *V. floribundum* extract.

TABLE 2: FTIR peaks for extract and nanoparticles.

Extract			Nanoparticles		
Peak name	cm <sup>-1</sup>		Peak name	cm <sup>-1</sup>	
1	3409.72	Vibrations of the -OH groups of phenolic moiety	a	3354.02	Vibrations (inter o intramolecular) of -OH groups of the phenolic
3	1594.46	C=C ring stretching in polyphenols	b	1634.98	C=C alkene conjugate cis and benzene ring
4	1405.43	In-plane bending vibration of -OH in phenol	c	1068.42	v sim. C-O ether forming ring or aryl ether
5	1070.42	v sim. C-O ether forming ring or aryl ether	d	630.23	Fe-O bond in stretching mode (tension)



The route of the petroleum hydrocarbon transformation can be as follows (Equations (4)–(8)) [33]:



where RH is the petroleum hydrocarbon compound with H<sup>+</sup> as the extractable proton and TPH\* and TPH are fraction of hydrocarbon radical and fraction of stable hydrocarbon, respectively.

## 4. Conclusions

According to TEM images, around 90% of nanoparticles prepared with *V. floribundum* show 5 to 25 nm in diameter regardless of the iron precursor concentration. The mineral content of the vZVI nanoparticles is 24% of alpha iron with a body-centered cubic crystal structure, and the remaining

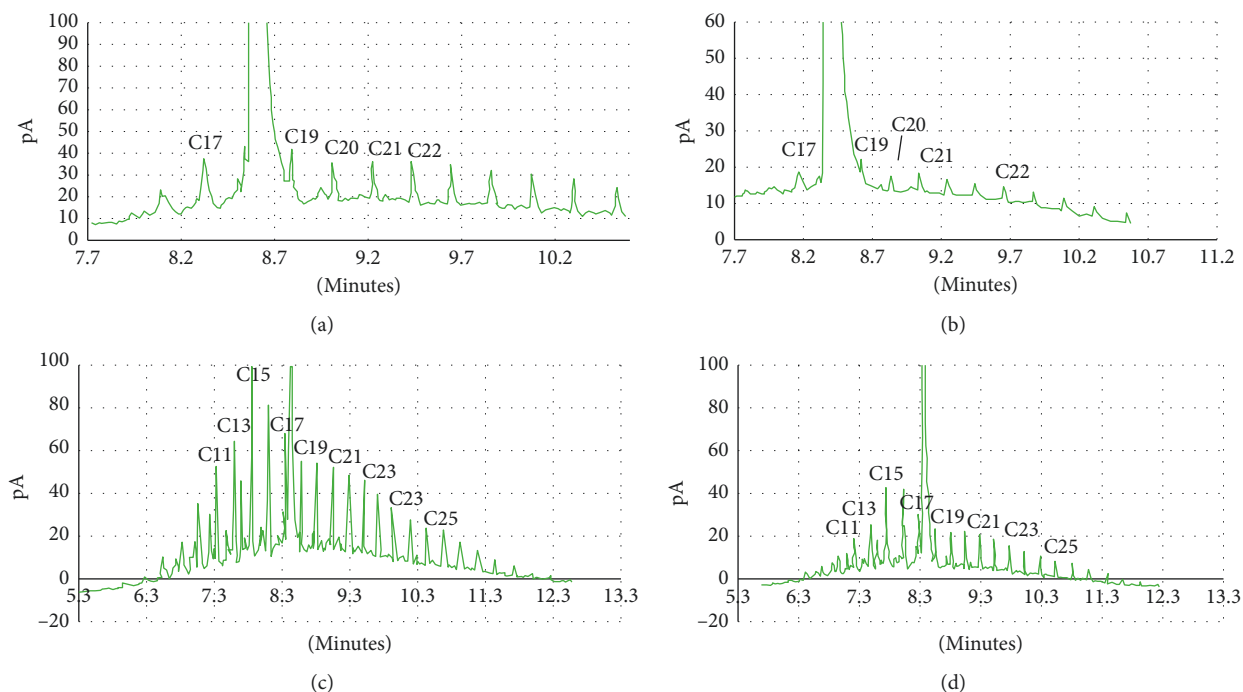


FIGURE 5: Chromatograms of TPHs derivatives in water before and after treatment with vZVI: (a) initial concentration = 9.32 ppm, (b) final concentration = 1.31 ppm, (c) initial concentration = 94.20 ppm, and (d) final concentration = 26.80 ppm.

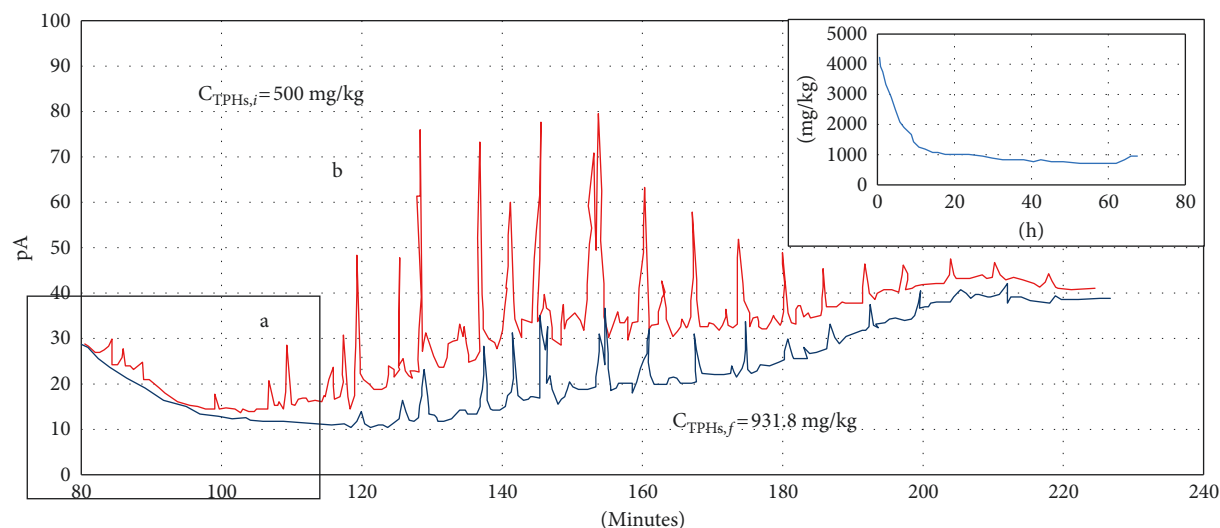


FIGURE 6: Chromatogram of TPHs derivatives: before and after treatment with vZVI.

fraction is composed of iron oxides. FTIR studies indicate  $-OH$  and  $C=C$  groups of the mortiño berry extract could have participated in the formation and stabilization of the iron nanoparticles. In general, the removal of TPHs with the Fe nanoparticles was successful as demonstrated by the chromatographic peaks of TPHs derivatives. Nevertheless, the treatment is strongly influenced by the content of iron in the nanoscale particles. Removals of 88.24% and 81.90% of petroleum hydrocarbons from water and soil samples were achieved after 12 min and 32 h of treatment with the vZVI particles, respectively. The good performance of vZVI

particles can be associated with their increased surface area, higher reactivity, the possibility of *in situ* treatment. Thus, this technique may be efficacious to be used in the remediation water and soil contaminated with petroleum hydrocarbons in less time compared to a conventional bioremediation process.

### Data Availability

The data used to support the findings of this study are available from the corresponding author upon request.

## Conflicts of Interest

The authors declare that they have no conflicts of interest.

## Acknowledgments

The authors acknowledge the assistance of Andrea Vaca with the TEM images, data processing, and XRD analysis. They thank Dr. Miguel Angel Bustamante Domínguez for his help in interpreting XRD spectra and the Universidad de las Fuerzas Armadas-ESPE for funding Project 2015PIC-004. Also, they show gratitude to all other contributors for providing us with the early data presented in the III International Congress of Nanoscience and Nanotechnology (ICNN'2017) held in Quito, Ecuador.

## References

- [1] G. Todd, R. Chessin, and J. Colman, *Toxicological Profile for Total Petroleum Hydrocarbons (TPH)*, U.S. Department of Health and Human Services, Washington, DC, USA, 1999.
- [2] X. Huang, Y. El-Alawi, J. Gurska, B. Glick, and B. Greenberg, "A multi-process phytoremediation system for decontamination of persistent total petroleum hydrocarbons (TPHs) from soils," *Microchemical Journal*, vol. 81, no. 1, pp. 139–147, 2005.
- [3] K. Masakorala, J. Yao, H. Guo et al., "Phytotoxicity of long-term total petroleum hydrocarbon-contaminated soil—a comparative and combined approach," *Water, Air, and Soil Pollution*, vol. 224, no. 5, p. 1553, 2013.
- [4] S. Gan, E. Lau, and H. Ng, "Remediation of soils contaminated with polycyclic aromatic hydrocarbons (PHAs)," *Journal of Hazardous Materials*, vol. 172, no. 2-3, pp. 532–549, 2009.
- [5] M. Chang, C. Huang, and H. Shu, "Effects of surfactants on extraction of phenanthrene in spiked sand," *Chemosphere*, vol. 41, no. 8, pp. 1295–1300, 2000.
- [6] M. Litter, A. Sancha, and A. Ingallinella, "Tecnologías económicas para el abatimiento de arsénico en aguas," in *Proceedings of Programa Iberoamericano de Ciencia y Tecnología para el Desarrollo*, Buenos Aires, Argentina, 2010.
- [7] B. Schrick, W. Hydutsky, J. Blough, and T. Mallouk, "Delivery vehicles for zerovalent metal nanoparticles in soil and groundwater," *Chemistry of Materials*, vol. 16, no. 11, pp. 2187–2193, 2004.
- [8] H. Gomes, L. Ottosen, A. Ribeiro, and C. Dias-Ferreira, "Treatment of a suspension of PCB contaminated soil using iron nanoparticles and electric current," *Journal Environmental Management*, vol. 151, pp. 550–555, 2015.
- [9] N. Mueller and B. Nowack, "Nanoparticles for remediation: solving big problems with little particles," *Elements*, vol. 6, no. 6, pp. 395–400, 2010.
- [10] D. O'Carroll, B. Sleep, M. Krol, H. Boparai, and C. Kocur, "Nanoscale zero valent iron and bimetallic particles for contaminated site of remediation," *Advances in Water Resources*, vol. 51, pp. 104–122, 2013.
- [11] S. Cook, *Assessing the Use and Application of Zero Valent Iron Nanoparticle Technology for Remediation at Contaminated Sites*, Jackson State University, Jackson, MS, USA, 2009.
- [12] C. Barreto, *Visión General de la Nanotecnología y Sus Posibilidades en la Industria de Alimentos*, ReCiTeIA, Cali, Colombia, 2011.
- [13] M. N. Nadagouda, A. B. Castle, R. C. Murdock, S. M. Hussain, and R. S. Varma, "In vitro biocompatibility of nanoscale zerovalent iron particles (NZVI) synthesized using tea polyphenols," *Green Chemistry*, vol. 12, pp. 114–122, 2010.
- [14] TULSMA, *Anexo 2 del libro VI del Texto Unificado de Legislación Secundaria del Ministerio del Ambiente: Norma de Calidad Ambiental del Recurso suelo y Criterios de Remediación para suelos contaminados*, TULSMA, Ecuador, 2015.
- [15] W. Brand-Williams, M. Cuvelier, and C. Berset, "Use of a free radical method to evaluate antioxidant activity," *LWT-Food Science and Technology*, vol. 28, no. 1, pp. 25–30, 1995.
- [16] M.-C. Chang, H.-Y. Shu, W.-P. Hsieh, and M.-C. Wang, "Using nanoscale zero-valent iron for the remediation of polycyclic aromatic hydrocarbons contaminated soil," *Journal of the Air and Waste Management Association*, vol. 55, no. 8, pp. 1200–1207, 2005.
- [17] M. Chang, H. Shu, W. Hsieh, and M. Wang, "Remediation of soil contaminated with pyrene using ground nanoscale zero-valent iron," *Journal of the Air and Waste Management Association*, vol. 57, no. 2, pp. 221–227, 2007.
- [18] M. C. Chang and H. Y. Kang, "Remediation of pyrene contaminated soil by synthesized nanoscale zero valent iron particles," *Journal of Environmental Science and Health Part A*, vol. 44, no. 6, pp. 576–582, 2009.
- [19] E. Murgueitio, L. Cumbal, A. Debut, and J. Landívar, "Synthesis of iron nanoparticles through extracts of natives fruits of Ecuador as capulí (*Prunus serotina*) and mortiño (*Vaccinium floribundum*)," *Biology and Medicine*, vol. 8, no. 3, p. 1, 2016.
- [20] C. Vasco, J. Ruales, and A. Kaml-Eldin, "Total phenolic compounds and antioxidant capacities of major fruits from Ecuador," *Food Chemistry*, vol. 111, no. 4, pp. 816–823, 2008.
- [21] S. Roldan, *Caracterización Molecular, Funcional y Estudio del Comportamiento Post Cosecha del Mortiño (Vaccinium floribundum Kunth) de la Comunidad de Quinticusig del Cantón Sigchos de la Provincia de Cotopaxi*, Escuela Politécnica Nacional, Quito, Ecuador, 2012.
- [22] S. Zapata, A. M. Piedrahita, and B. Rojano, "Capacidad atrapadora de radicales oxígeno (ORAC) y fenoles totales de frutas y hortalizas de Colombia," *Perspectivas en Nutrición Humana*, vol. 16, no. 1, pp. 25–36, 2014.
- [23] V. Roshchina, *Model Systems to Study the Excretory Function of Higher Plants*, Springer, Berlin, Germany, 2014.
- [24] G. Ortega, A. Bermello, M. Guerra, G. Castillo, S. Armenteros, and G. Miere, "Estudios de separación y caracterización de pigmento en caldo de fermentación Botryodiplodia theobromae," *ICIDCA. Sobre los Derivados de la Caña de Azúcar*, vol. 41, no. 3, pp. 27–34, 2007.
- [25] A. Castañeda-Sanchez and J. Guerrero-Beltrán, *En los Espectros FTIR de Ambas Fracciones*, Tema Selectos de Ingeniería en Alimentos, Puebla, PUE, Mexico, 2015.
- [26] C. Arroyo, A. Debut, C. Stael, K. Guzman, and B. Kumar, "Reliable tools for quantifying the morphological properties at the nanoscale," *Biology and Medicine*, vol. 8, no. 3, p. 281, 2016.
- [27] S. Steven, H. Genuino, M. Nashaat, S. Mohammad, L. Zhu, and G. Hoag, "Green synthesis of iron nanomaterials for oxidative catalysis of organic environmental pollutants," in *New and Future Developments in Catalysis: Catalysis for Remediation and Environmental Concerns*, Elsevier, New York, NY, USA, 2013.
- [28] M. Abril, H. Ruiz, and L. H. Cumbal, "Biosynthesis of multicomponent nanoparticles with extract of mortiño (*Vaccinium floribundum Kunth*) berry: application on heavy metals removal from water and immobilization in soils," *Journal of Nanotechnology*, vol. 2018, Article ID 9504807, 10 pages, 2018.

- [29] P. Palacios, L. De los Santos Valladares, A. Bustamante, and J. González, "Estudio de la deshidroxilación en el óxido férrico hidratado denominado limonita," *Revista Sociedad Química del Perú*, vol. 78, no. 3, pp. 198–207, 2012.
- [30] F. Osorio, J. Torres, and M. Sánchez, *Tratamiento de Aguas Para la Eliminación de Microorganismos y Agentes Contaminantes*, Dias de Santos, Madrid, Spain, 2010.
- [31] S. Chitra, K. Paramasivan, P. Sinha, and K. Lal, "Ultrasonic treatment of liquid waste containing EDTA," *Journal of Cleaner Production*, vol. 12, no. 4, pp. 429–435, 2004.
- [32] P. Ghosh, A. Samanta, and S. Ray, "COD reduction of petrochemical industry wastewater using Fenton's oxidation," *Canadian Journal of Chemical Engineering*, vol. 88, no. 6, pp. 1021–1026, 2010.
- [33] A. Rubio, E. Chica, and G. Peñuela, "Aplicación del proceso Fenton en el tratamiento de aguas residuales de origen petroquímico," *Ingeniería y Competitividad*, vol. 12, no. 2, pp. 211–223, 2014.



